edgeFLEX

D5.3

Report on field trial of frequency, inertial response and dynamic-phasor driven voltage control concepts in Italy

The research leading to these results has received funding from the European Union's Horizon 2020 Research and Innovation Programme, under Grant Agreement no 883710.

Project Name	edgeFLEX
Contractual Delivery Date:	31.03.2023
Actual Delivery Date:	31.03.2023
Author(s):	RWTH – UNIBO
Workpackage:	WP5 – Field Trials of Dynamically Controlled VPP Solutions
Security:	P
Nature:	R
Version:	V1.0
Total number of pages:	36

Abstract

The deliverable describes the design, the development, and the operation of the Italian field trial. Instrument transformers and PMUs (commercial and prototypes) have been deployed in the live distribution network of Unareti, to collect measurements for the edgeFLEX edge control algorithms to be tested. The deliverable, though, is divided in two main sections. The first section focuses on the design and development of the trial. The second section presents the results of the application of the implemented edge algorithms.

Keyword list

Field trial, distribution network, voltage control, instrument transformers, PMUs

Disclaimer

All information provided reflects the status of the edgeFLEX project at the time of writing and may be subject to change.

Executive Summary

An important aspect of algorithm development is its implementation in real-world scenarios. While laboratory simulations provide a preliminary validation of new concepts, they do not account for all potential situations that may arise in a field trial in a live network. WP5, however, focuses on testing edge algorithms in live portions of commercially operated distribution networks.

In particular, the Italian field trial takes place at the facilities of one of the major Italian DSOs, Unareti, who joined the edgeFLEX project at their own expense, as demonstrators of the developed solutions during the second half of the project. The field trial and its results, described in this deliverable, began with the design of the distributed measurement system (DMS) needed to obtain the necessary measurements for the edge algorithms. Following the design work, laboratory tests and simulations were carried out to make a preliminarily test of the validity of the design solutions. Once the trial was fully operational, a complete assessment of the solutions became possible. The assessment of the solutions and conclusions of the field trial are described in the final chapters of this deliverable.

Authors

Partner	Name	e-mail
RWTH		
	Edoardo De Din	ededin@eonerc.rwth-aachen.de
	Manuel Pitz	manuel.pitz@eonerc.rwth-aachen.de
UNIBO		
	Alessandro Mingotti	alessandro.mingotti2@unibo.it
	Roberto Tinarelli	roberto.tinarelli3@unibo.it
	Lorenzo Peretto	lorenzo.peretto@unibo.it
	Gaetano Pasini	gaetano.pasini@unibo.it
	Federica Costa	federica.costa2@unibo.it

Table of Contents

1. Introduction

This deliverable summarizes the activities carried out during the edgeFELX Italian field trial developed. The trial aimed to implement and evaluate the fast dynamic service developed in edgeFLEX in a live power network, to support and confirm the VPP concepts developed by the project.

Objective of the report

The report aims to provide a detailed description of the main activities involved in running this fully operational field trial. It starts by outlining the equipment needed at the trial facilities before moving on to the technical part of the report, which covers tests and simulations. Overall, the report aims to provide a realistic overview of the field trial implementation from the perspectives of both the DSO and of the edgeFLEX consortium.

1.1 Outline of the report

The report begins by presenting the objectives of the trial. It then introduces the DSO hosting the trial, followed by a description of the trial location and grid. The technical section of the report covers the trial requirements and preliminary tests performed on the equipment to be used in the trial. Finally, the tests and simulations conducted during the trial are presented and discussed.

1.2 How to Read this Document

This report can be read as a standalone document. However, other deliverables can be helpful to get a better view of the concepts advanced in the edgeFLEX project. In particular, other deliverables closely related to this one are:

- D1.1 - Scenario description for dynamic-phasor driven voltage control for VPPs (M12): This deliverable starts with an overview of the state of the art in terms of VPPs and of services developed within their framework. Moreover, D1.1 introduces to the reader the dynamic-phasor driven voltage control scenario and the technical terminology adopted through the entire edgeFLEX project, and
- D4.1 - Description of EdgeFLEX platform design (M12): This deliverable describes the overall edgeFLEX platform where the voltage control is placed as service.

2. Trial description and objectives

This chapter introduces the Italian trial and its characteristics. First, the DSO hosting the trial is presented in Section 2.1. Then, the technical characteristics are detailed in Section 2.2.

2.1 The DSO: Unareti

2.1.1 Introduction

Unareti is the only company providing integrated and widespread network services for the distribution of electricity and gas. With over 1,500 employees and a turnover of more than 600 million euros, they operate in about 200 Italian municipalities across 7 regions, with more than 20,000 km of network. Their goal is to achieve a more flexible use of resources and obtain management synergies on a multi-service model, resulting in lower costs and better services through professionalization and skill enhancement. By integrating previously separate businesses, Unareti will be able to accelerate technological development and make the most of the evolution of smart grid technologies to guarantee efficient and quality services to citizens and the territories in which they operate.

2.1.2 The electricity distribution

The activity of distributing electricity is a public service exercised under concession, according to criteria of neutrality, transparency, and effectiveness towards sales companies, as well as efficiency in management to reduce costs and therefore distribution tariffs to customers. It is regulated by the ARERA (Law No. 481 of 14 November 1995). The ARERA, with resolution 11/07 as amended, also imposed the application of obligations about functional, administrative, and accounting unbundling for the distribution of gas.

The distribution activity is therefore placed within the broader chain of the liberalized electricity market which includes the production, importation, transmission, and distribution dedicated to linking the supply sources to the final user customers and the sale to end customers. The electricity distribution activity includes the operations of management, operation, maintenance, and development of the high, medium, and low voltage electricity distribution networks, entrusted under concession in a territorial area of competence to the owner distribution company of the concession, including the physical operations of suspension, reactivation and disconnection and the activities of a commercial nature connected with the provision of the distribution service.

The electricity distribution network includes medium voltage power lines (between 10 and 20 kV) and low voltage lines (below 1000 V, normally 400 V), HV/MV transformation plants (primary substations), pole-mounted transformers or medium voltage electrical substations (LV/MV secondary substations), disconnectors and switches, measuring instruments. On the other hand, the high voltage lines (between 60 and 400 kV) are generally part of the transmission grid managed by the only national operator (Terna).

The distribution activity also includes the metering service, i.e., the organizational, processing, IT and telematic operations, aimed at determining, detecting, making available and archiving the validated metering data of the electricity fed into and withdrawn from the distribution networks, both where the source of this datum is a measuring device, and where the determination of this datum is also obtained conventionally through the application of numerical algorithms. It also includes operations related to interventions on the meters resulting from contractual changes or management of the commercial relationship, which do not require the replacement of the meter.

2.1.3 Sustainability

Sustainability is a core value for Unareti, which strives to manage risks and mitigate the impacts of its activities while creating value for all stakeholders. The company is guided by principles of excellence in results, responsibility, competence and determination, team spirit, innovation, and sustainability as outlined in the A2A group's Code of Ethics. Unareti pays close attention to the impact of its decisions on the environment and communities and adopts the best technologies to manage its activities. The company's business model integrates these principles into its strategies, promoting economic growth and enhancing its image. Unareti is committed to promoting respect for people, the environment, and the interests of the territories in which it operates while creating development opportunities for both the communities and the industrial realities present. The company's culture values a balance between economic success, environmental protection, and social responsibility.

2.2 The Unareti field trial in edgeFLEX

2.2.1 Location and Smart Lab

The Italian trial takes place at one of Unareti's facilities in Milan (Figure 1), specifically in the Smart Lab, a new building dedicated to innovative projects.

Figure 1 Italian trial location in the geographical map

What is the Smart Lab

The Smart Lab serves as a space for experimenting, monitoring, and managing the electricity grid, enabling the Smart Grid to improve the grid's operational standards and make it more sustainable and effective, both locally and for the entire system. The Smart Lab is equipped with a real-time monitoring and remote-control system that detects the strategic parameters of the network and automatically selects faults to improve the quality and continuity of the service.

Control room

The control room is the area of the Smart Lab where operators interface with the intelligent electronic devices of the network (IED) through a Human Machine Interface (HMI) station connected to a local control, supervision, and data acquisition system (SCADA). The SCADA graphically represents all the information received from the devices. This room communicates with the Unareti Remote Control Center ADMS (Advanced Distribution Management System) through the IEC60870-5-104 protocol, a dedicated communication system for telecontrol between local SCADAs and remote telecontrol centers.

Smart Lab electrical network

The Smart Lab controls a portion of grid consisting of five main sections, each representing a secondary substation equipped with high-tech tools to achieve efficiency goals and improve grid performance. One of the primary objectives is to automate the system as much as possible, ensuring its protection and restoration in the event of a failure by leveraging real-time information exchange between intelligent devices and Remote-Control Centers, both local and remote. The secondary cabins contain the following components:

- MV section made up of compartments connected through an MV busbar system, which can vary based on functionality.
- MV/LV oil transformer used to transfer power and reduce voltage levels.

- LV section comprising of switch disconnectors and/or switches connected to the LV bus to power and protect LV lines and monitor electrical quantities, which are sent to the Remote Terminal Unit (RTU) or Edge Device.
- Remote control consisting of an RTU and/or Edge Device, power supply and batteries, 4G modem or fiber optic connection (FO) router for real-time data exchange with the Remote Control Center.
- Protection system consisting of one or more IEDs that can process electrical quantities and automatically intervene on the faulty section of the network, isolating the affected area. The IEDs can communicate with other IEDs installed in different substations using the IEC61850 protocol and communication vectors.

Automation and Monitoring

To achieve this, secondary substations are strategically connected, and switch compartments are equipped with sensors connected to the IEDs, which can perform protection and control functions. In case of a fault, the IEDs that detect the fault send block messages to the communication network via Gooses (Generic Object-Oriented Substation Events). The other IEDs, capable of receiving these messages, accept them, and quickly block their protection functions, preventing the opening of the switches. This all happens automatically, in one second, isolating the faulty portion of the network.

2.2.2 Portion of grid considered in the field trial

Figure 2 shows a simple electric schematic of the portion of the grid monitored by the Smart Lab. Note that the portion of the grid used in the trial is not dedicated to academic projects or testing; it is part of the actual grid supplying electricity to the city, feeding a variety of different customers (industrial and private) and receiving power from renewable energy sources connected to the feeders.

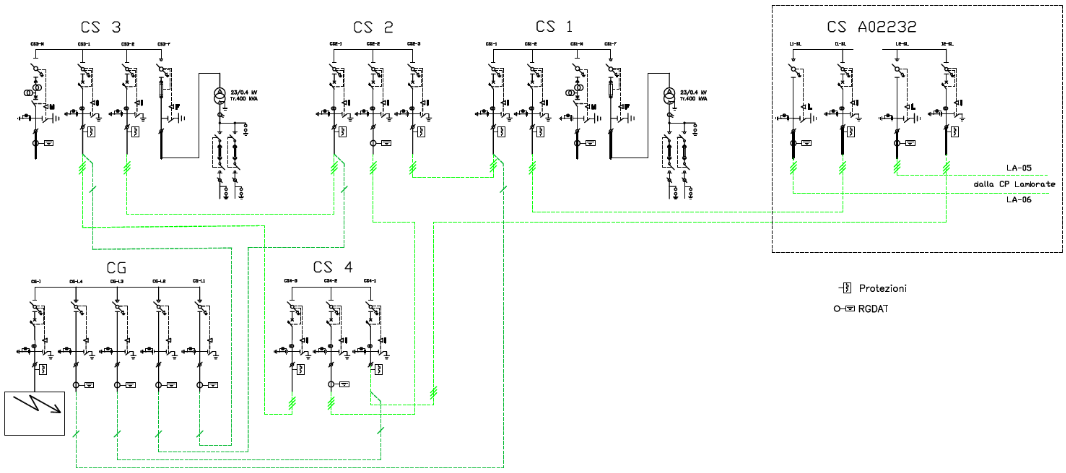

Figure 2 Electrical schematic of the portion of grid considered

2.2.3 Objectives of the trial

The Italian trial was equipped with two types of edge devices: the edgePMU provided by partner RWTH and a commercial PMU purchased at Unareti's expense (no funds were given to Unareti during the project). The objectives of the Italian trial were as follows:

- To compare innovative prototype edgePMUs with commercial ones,
- To demonstrate the exploitability of edgePMUs in distribution networks,
- To increase network observability through the synchronization and high reporting rate features of the edgePMU,
- To deploy the edgeFLEX fast dynamic services in actual electric grids, and
- To validate the edgeFLEX platform within one of the largest Italian DSOs.

2.2.4 Link to the other WPs

The success of the Italian field trial and that of WP5 depended on the work carried out in the other WPs. The theoretical concepts developed in WP1, WP2, and WP3 were implemented in the trial. WP1 played a significant role in the trial's success due to its nature as a work package with the objective of providing improved voltage control algorithms and solutions. The results of WP4, which integrated the implemented components of the research oriented work packages 1-3, were essential in building the framework around the trial and the data it generated. The trial's results were a critical input for the dissemination activities within WP7 and the standardization proposals written in WP6.

3. Developing the field trial

3.1 Description of the distributed measurement system

The measures collected in the field are the essential input of every ancillary service developed for smart grids. Therefore, performing good measurements is a crucial activity. The measurement setup designed for the Italian trial is depicted in Figure 3.

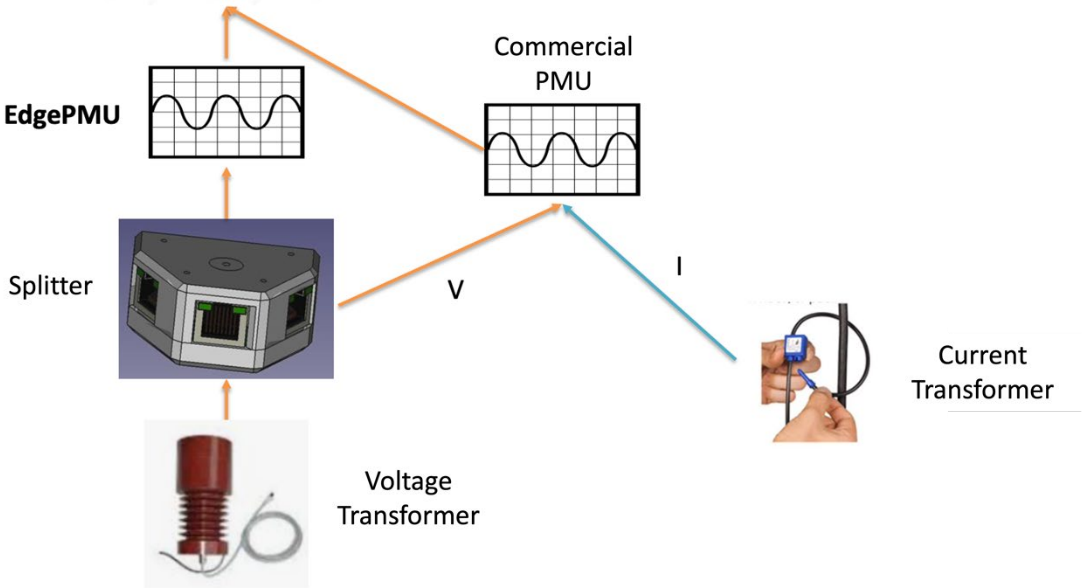

Figure 3 Measurement setup designed and used in the Italian trial

The setup consists of:

- A three-phase system of voltage and current transformers. They are used to sense the voltages and the current of the node/branch in which they are installed. The voltage transformer (VT) belongs to the low-power technology family, and it is active. The current transformer (CT) also belongs to the low-power technology family, but it is passive. The CT is a Rogowski coil sensor.
- A passive splitter. It is used to split the voltage signal so that it can be collected by two different devices simultaneously. Being passive, the splitter doesn't need a power supply, reducing its impact on the overall measurement setup.
- The edge devices. One edge device is the edgePMU developed by RWTH. The other is a commercial PMU for MV networks.

In general, voltage and current data are gathered and transmitted to the edge devices (with only current data sent to the commercial device). The edge devices then process the electrical quantities before forwarding them to the data concentrator.

The measurement setup employed permits the acquisition of data for any ancillary service, although during the Italian trial, only the voltage control service was tested for two reasons:

- Firstly, the frequency control service is significant only when considering a large portion of the network. The edge device used is capable of correctly measuring frequency, but in the section of the grid considered in this field trial, frequency estimation would not have provided any additional information.
- Secondly, the inertia estimation service was not implemented or tested due to the nature of the grid. An MV portion of the distribution network provided for the field trial was not an appropriate location for estimating inertia. Once again, a larger portion of the network involving power generation assets (and hence, also the transmission network) would have been more suitable for the implementation of this service.

3.2 Laboratory testing and validation of the setup

3.2.1 Introduction

This section describes in a simple way how to test a measurement chain like the one described in Section 3.1. The characterization tests presented in the following aim at verifying the accuracy performance of the setup. Therefore, the results can be used for further consideration in any application exploiting the measures obtained from the measurement setup.

3.2.2 The characterization process and setup

To characterize the edgePMUs and instrument transformers, only one device is needed for measuring purposes: a synchronized reference source of voltage and current, also known as a calibrator. The calibrator can directly feed the edgePMU if specific performance assessment is required. Alternatively, it can feed the instrument transformer and the edgePMU chain for observing overall performance. The two slightly different solutions are depicted in Figure 4.

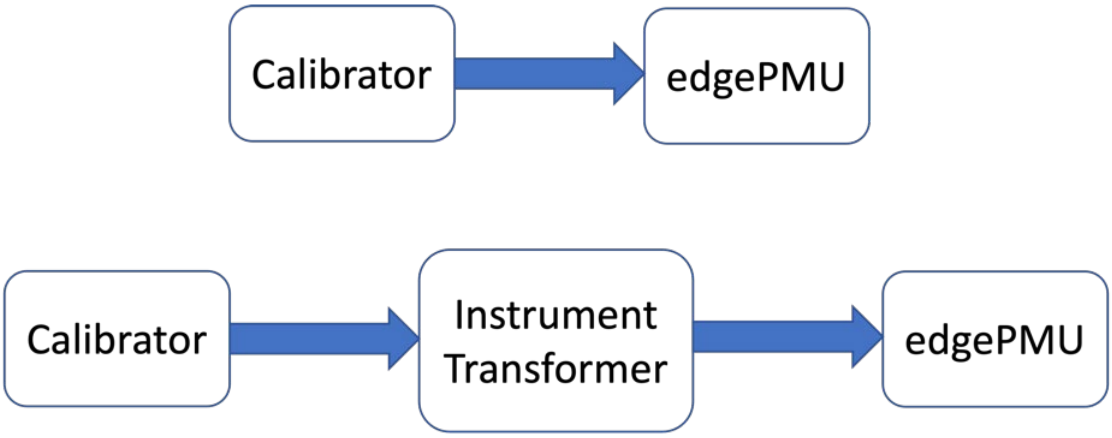

Figure 4 Two characterization setups used to test the edgePMU and the instrument transformers

The setup shown in the picture was used to perform the following tests:

- Test versus frequency: The frequency was varied in the range of ± 1% of the rated frequency, with 0.1 Hz steps, while the rated voltage was maintained. In each step, 100 measurements were taken to obtain a mean value. The applied signal did not contain any other frequency components. The objective of this test was to verify voltage stability when the frequency varies within the limits set by the standards[1] [EN 50160].
- Test vs. harmonics. Odd harmonic components were superimposed on the ideal 50 Hz signal at the rated voltage and frequency, one at a time. For each test, 100 measurements were taken. The amplitude of the superimposed harmonic component was taken from the maximum values specified in the relevant standard [EN 50160].

3.2.3 The characterization results

The results of the test vs. frequency are shown in Figure 5. The voltages are expressed in p.u. for the sake of clarity. The results clearly demonstrate the edgePMU correct estimation of the voltage when the frequency is varying. In fact, maximum measured deviations are in the order of few parts per thousand.

[1] EN 50160:2017. Voltage Characteristics of Electricity Supplied by Public Electricity Networks; European Committee for Standardization: Brussels, Belgium, 2017.

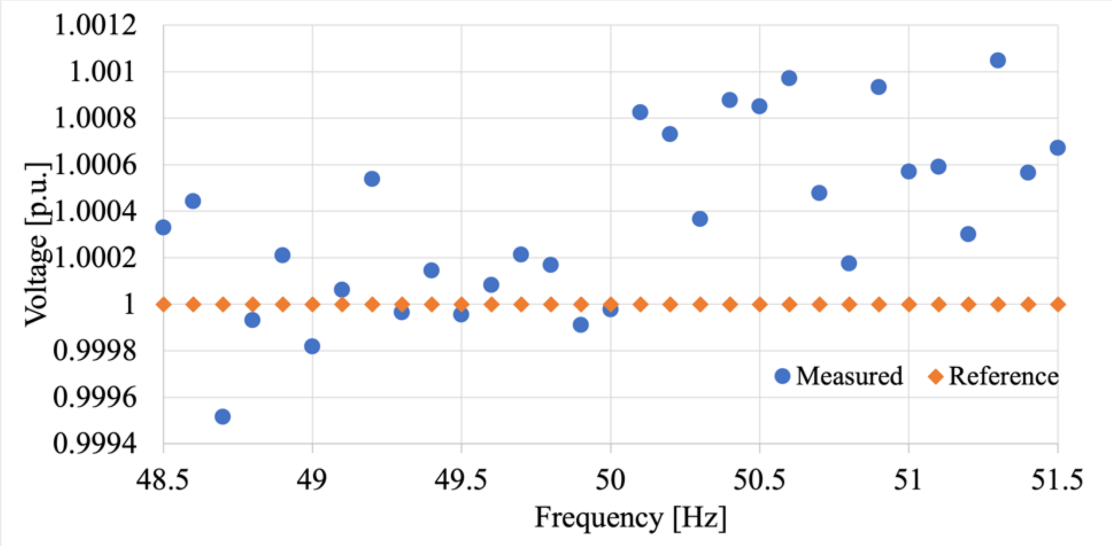

Figure 5 Results of the frequency test

The results of the test vs. harmonics are shown in Figure 6. On the x-axe the order of the harmonic superimposed to the 50 Hz signal is given. The results, compared to the reference source, show how well the edgePMU, even with the instrument transformers in cascade, extract the harmonic components from the measured signal. Such a capability allows the operators to implement any kind of power quality application.

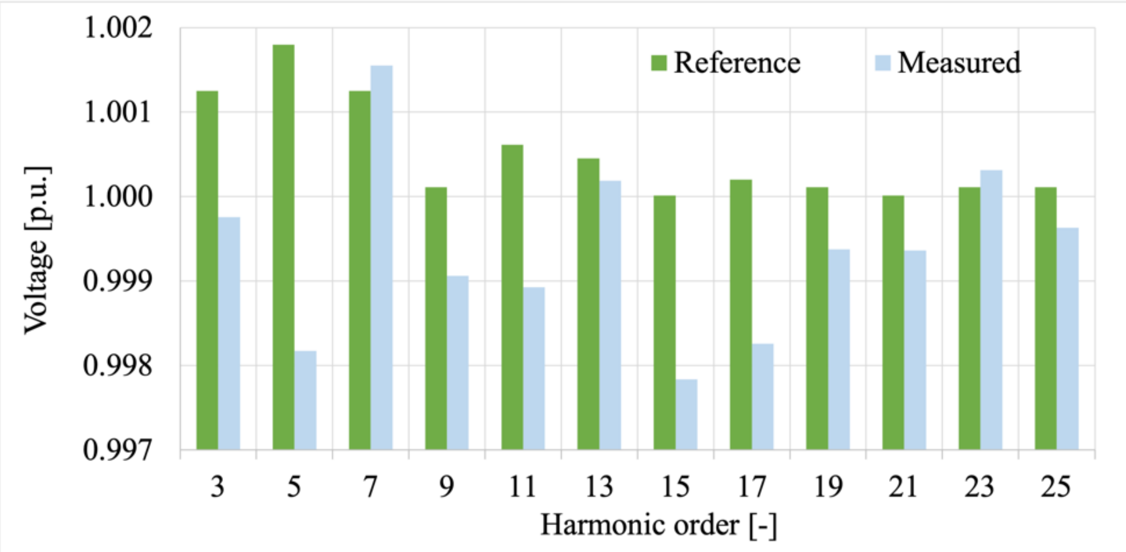

Figure 6 Results of the harmonic test

From both set of test results, it can be concluded that the voltage control service would efficiently run thanks to the performance of the considered measurement chain.

3.3 5G availability at the trial location

After identifying the locations for deploying the edgeFLEX edgePMUs in the Unareti field trial, EDD and UniBo, along with A2A, approached the public mobile operator TIM to determine the availability of 5G coverage at the field trial sites in Milan. Despite several discussions over many months, TIM was unable to provide a timeline for when 5G coverage would be available at the relevant field trial sites. Therefore, cabled networks and 4G were used for communication in the field trial deployments.

4. Implementation of the distributed voltage control service in the trial

4.1 Objective of the voltage control in the field trial

The objectives of the distributed control implementation in the Italian field trial can be summarized as follows:

- Collection of the edgePMUs measurement data,
- Integration of the edgePMUs measurements in the simulation environment,
- Implementation of the distributed voltage control algorithm,
- Development of the Cyber Physical System and instantiation with software containers, and the
- Test of the field trial in terms of coordination of the resources, scalability and interaction of DSO and Customer's assets

4.2 Implementation of the field trial

This section discusses the implementation of the field trial, including the integration of measured data in the simulation environment, the grid model used for testing, the algorithm description, and the software container implementation. Due to the small size of the grid under test and the absence of controllable devices in the field, a simulated model was incorporated into the field trial grid model, and real measurements were integrated into the simulation. A distributed control algorithm was implemented and instantiated in a Cyber Physical System (CPS) using software containers.

4.2.1 Model of the grid

The Unareti grid test, referred to as the "A2A MV Field Test Grid," consists of four secondary substations which are electrically connected, as shown in the figure, and in which the edgePMUs have been installed. The data from this portion of the MV grid is presented in Table 4, in which the data has also been converted to per-unit values to comply with the power flow simulator input data.

However, it is apparent from the table that the A2A MV Field Test Grid alone is not sufficient to produce such a significant variation in voltage that the implementation of the voltage control algorithm would be required. This is due to the fact that, according to the branch-flow model, the voltage variation along the radial distribution grid is proportional to the impedance matrix of the grid itself (De Din, Pau, Ponci, & Monti, 2007) (Farivar).

Therefore, the original grid has been extended with an additional grid based on the well-known CIGRE benchmark MV grid (Resources, 2018), consisting of 15 nodes in a radial configuration described in Table 5. As illustrated in Figure 7, Energy Storage Systems (ESSs) and Photovoltaics (PVs) are connected to some of the nodes of the grid. These nodes, which are simulated, are fully controllable, allowing the control signals received by the control algorithm to modify the voltage profiles. This permits the control algorithm to be adequately tested in a simulated environment without posing a risk to the real system.

Since the A2A Field Test Grid does not have any connected controllable devices, the controllable PVs and ESSs are placed only in the CIGRE MV Grid. The locations of the controllable devices are described in Table 1.

Table 1 Position of PVs and ESSs

	PV	ESS
Node	7,11,12,13,14,15	7,11,13,14,15

Overall, the grid under test consists of 15 nodes, four of which are directly monitored with the installed edgePMUs while the others are simulated using a powerflow simulator (PYPOWER). As previously described, the edgePMUs installed in the Unareti grid are connected to the medium voltage side of the transformers located in the secondary substations. However, to simplify the integration of the measured data with the simulation environment, the measurement data is converted into per unit values.

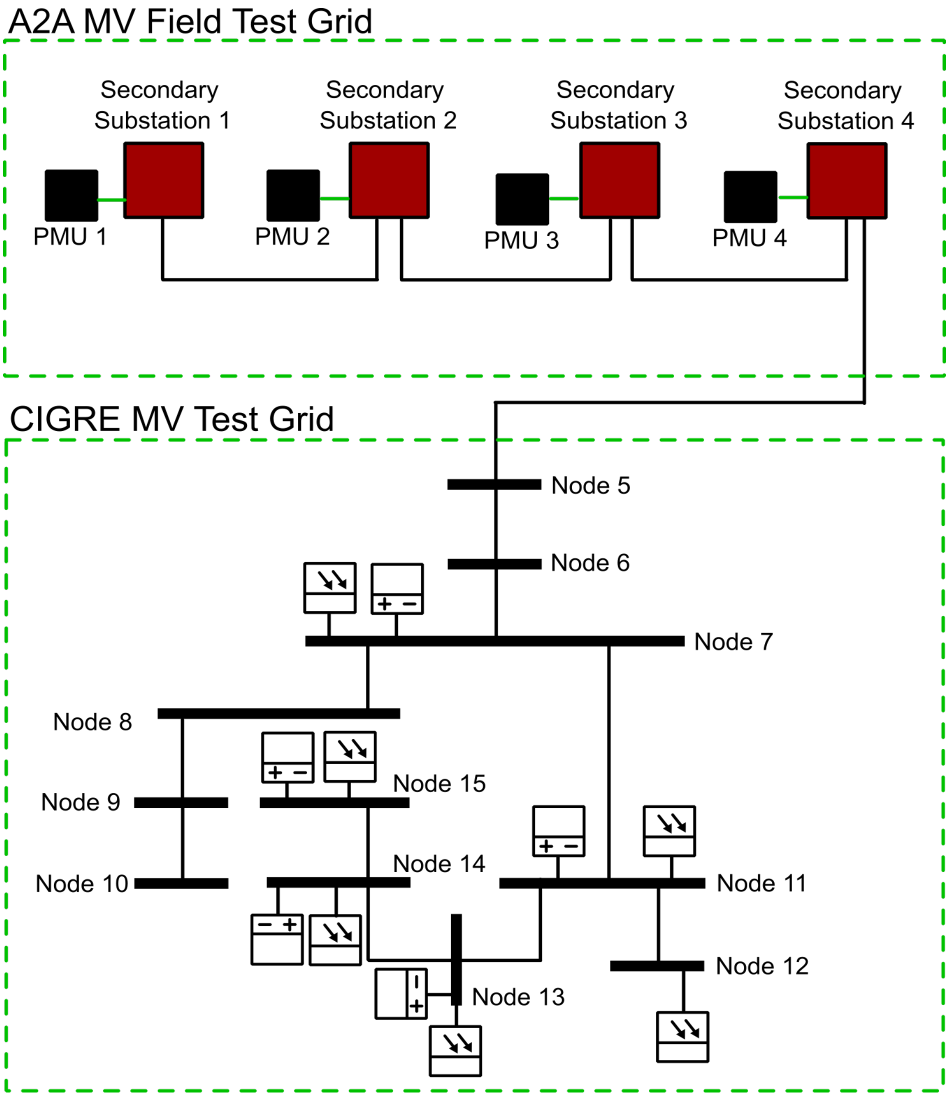

Figure 7 Model of the grid for the field trial

4.2.2 Integration of the edgePMUs data

The different edgePMU devices are connected to the local edge server via Ethernet and can eventually be connected to the internet via an LTE connection. Due to security limitations of the grid operator, the setup has not been connected to the local substation network. Instead, a dedicated virtual private network has been created to remotely control the edgePMUs. This network configuration is also used to initiate tests when needed and perform remote supervision of the devices. A user interface has been implemented to visualize the status of the installed edgePMUs, as shown in Figure 8, which displays a screenshot of the status of one edgePMU. Since each edgePMU is equipped with a GPS receiver, the data received by the devices also reports their locations. This is used to visualize the location and status of all edgePMUs on the location dashboard, as shown in Figure 9.

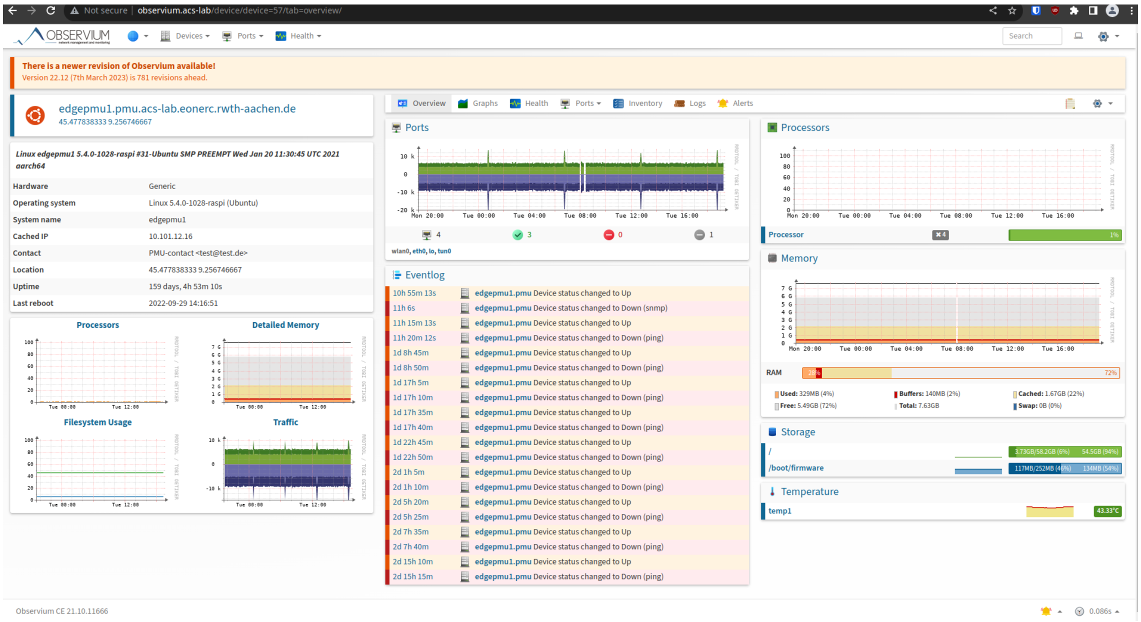

Figure 8 edgePMU1 monitoring

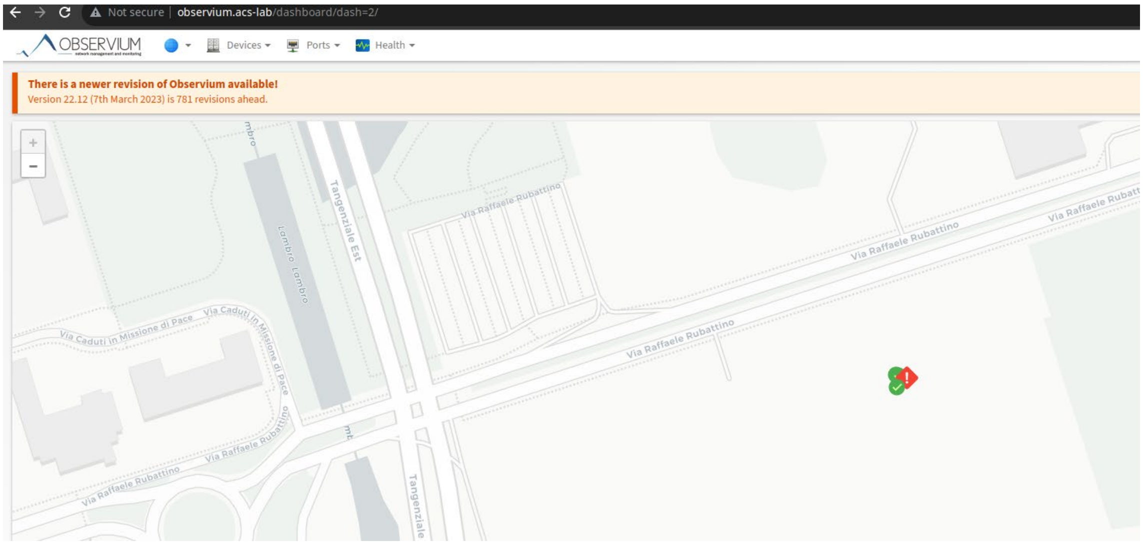

Figure 9 edgePMU status and location

4.2.3 Description of the algorithm

The distributed control implemented in the field trial refers to the one presented in (E. De Din). For a control variable x, which can be a vector of active or reactive power set-points for DGs or ESSs, and for V the voltage vector, the optimization problem is defined as:

$$\max_{x} x^T W x$$

$$s.t.\quad V_{min} \leq V \leq V_{max}$$

$$x_{min} \leq x \leq x_{max}$$

where W is real or imaginary part of the impedance matrix of the electrical grid.

The original problem is converted into the dual equivalent:

$$\mathcal{L} = x^T W x + \Lambda_{min}(V_{min} - V) + \Lambda_{max}(V - V_{max}) + X_{min}(x_{min} - x) + X_{max}(x - x_{max})$$

where $\Lambda_{min}, \Lambda_{max}, X_{min}, X_{max}$ are the vector of lagrangian multipliers associated to the constraints.

The dual ascent method is applied to the dual problem as follows:

$$\Lambda_{min}(k+1) = \Lambda_{min}(k) + \boldsymbol{\alpha}(V_{min} - V(k))$$
$$\Lambda_{max}(k+1) = \Lambda_{max}(k) + \boldsymbol{\alpha}(V(k) - V_{max})$$
$$X_{min}(k+1) = X_{min}(k) + \gamma(x_{min} - x(k))$$
$$X_{max}(k+1) = X_{max}(k) + \gamma(x(k) - x_{max})$$

And the minimization of the primal variable results in:

$$x(k+1) = -\left(\Lambda_{max}(k+1) - \Lambda_{min}(k+1)\right) - G(X_{max}(k+1) - X_{min}(k+1))$$

The matrix $G = W^{-1}$ is sparse, with a structure that directly depends on the topology of the grid, as described in Figure 10:

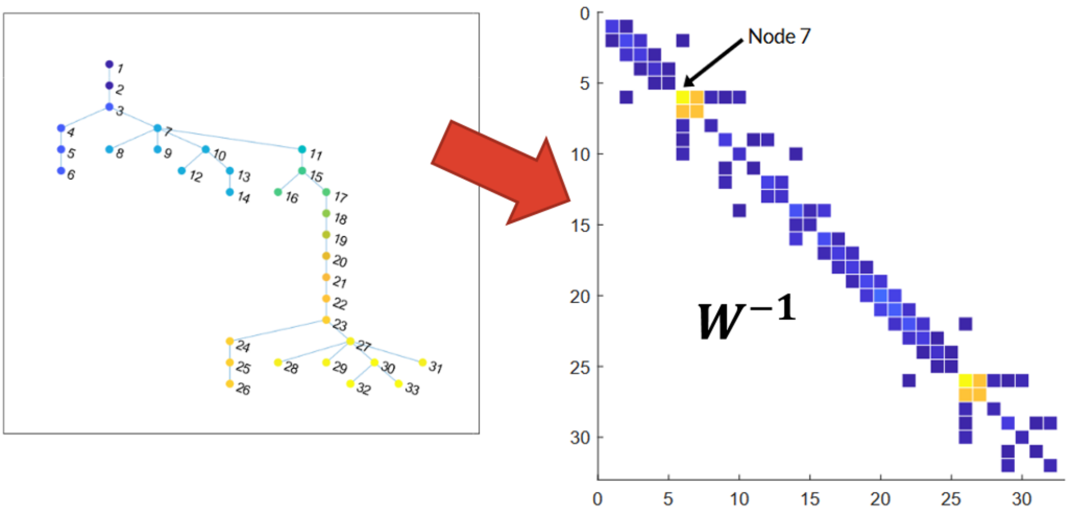

Figure 10 Sparse structure of the matrix W^{-1}

Due to the sparsity of the matrix, the calculation of the control output only depends on the exchange of lagrangian multipliers among the neighboring nodes.

Therefore, in the distributed control the data exchanged among the controllable nodes are values that cannot be directly linked with the private customer data. Moreover, the distributed implementation of the control makes the overall system more reliable, given that it does not represent a single point of failure. Both aspects are considered very critical for the European Commission (Commision, 2022), particularly in light of the growing number of cyber and physical attacks happening on the power grid (Council) (POLITICO).

The presented control algorithm has been implemented in a distributed architecture based on Docker containers (Docker, 2022), presented in the next section.

4.2.4 Implementation of the distributed control algorithm with software containers

The implementation of the distributed control algorithm is presented in this chapter, showing how the Docker-based environment to realize the so-called Cyber Physical System (CPS), described in Figure 11.

The CPS is made of three components:

- **Physical layer:** consisting of the distribution grid infrastructures, which include ESSs, DGs, loads and lines.
- **Graph layer:** provides a graph representation in terms of nodes and edges of the electrical grid, where the nodes are the electrical nodes where DGs or ESSs are installed, and the edges are the electrical lines.
- **Cyber layer:** comprises the intelligent nodes, which exchange data with their neighbours and execute the local optimization.

In the cyber layer the intelligent nodes of the distributed system are defined as *Clients* and the additional element that control the status of the control nodes and provides initialization data is defined as *Supervisor*.

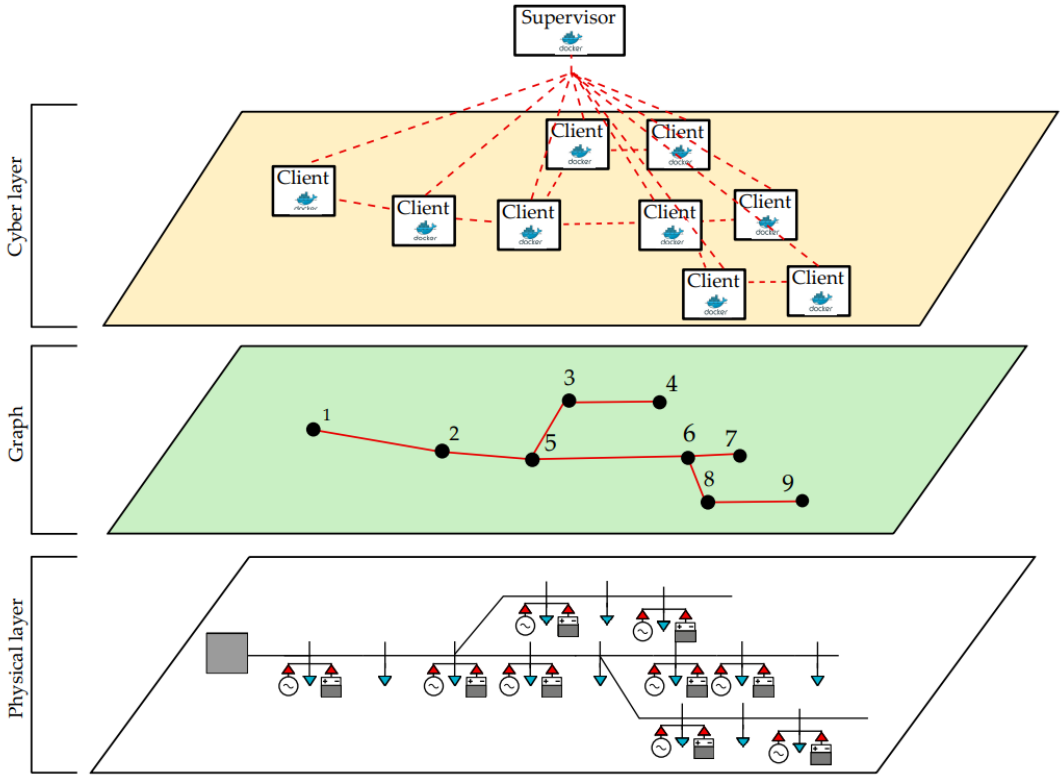

Figure 11 Description of the envisioned CPS system

To create a CPS system for the field trial, the Clients and the Supervisor have been implemented as software containers, which constitute a separate software element that can be integrated into the platform. As mentioned in the previous section, the distributed algorithm requires the exchange of Lagrangian multipliers to calculate the resulting control output. In this approach, this has been implemented using the HTTP protocol, which is represented by the red dashed lines in Figure 11 and defines the communication links based on the graph.

Since the control of the resources is only implemented in the portion of the grid simulated with the powerflow, the resulting scheme is shown in Figure 12. The figure illustrates how the measurements of the physical layer are integrated into the powerflow simulator by linking the received data with the simulation of the first four nodes of the grid. As previously mentioned, the measurement data from the physical grid are obtained through the installed edgePMUs, which transmit the measurements via the MQTT protocol. Therefore, the powerflow software subscribes to the topics of the edgePMUs to read the voltage measurements.

The overall simulated grid described in Section 4.2.1 includes six nodes where both PVs and ESSs or only PVs are installed. Therefore, six Client software containers are instantiated and linked based on the communication graph. The algorithm used to generate the graph is based on the inverse of the real and imaginary part of the impedance matrix and the software tool NetworkX (NetwrokX). The resulting algorithms are described in Annex A.1.2.1 and A.1.2.2. The simulated data and the control set-points are exchanged between Clients and powerflow using the HTTP protocol, represented by the green dashed lines in Figure 12.

The variables controlled by the distributed algorithm are the reactive power of the PVs (Q) and the active power control of the ESSs (P_{ESS}). Therefore, the matrix W can be substituted with:

- $X = \mathfrak{I}\,(Z)_{|PV}$, the imaginary part of the impedance matrix only considering the position of the installed PVs
- $R^{ESS} = \mathfrak{R}(Z)_{|ESS}$, the real part of the impedance matrix only considering the position of the installed ESSs

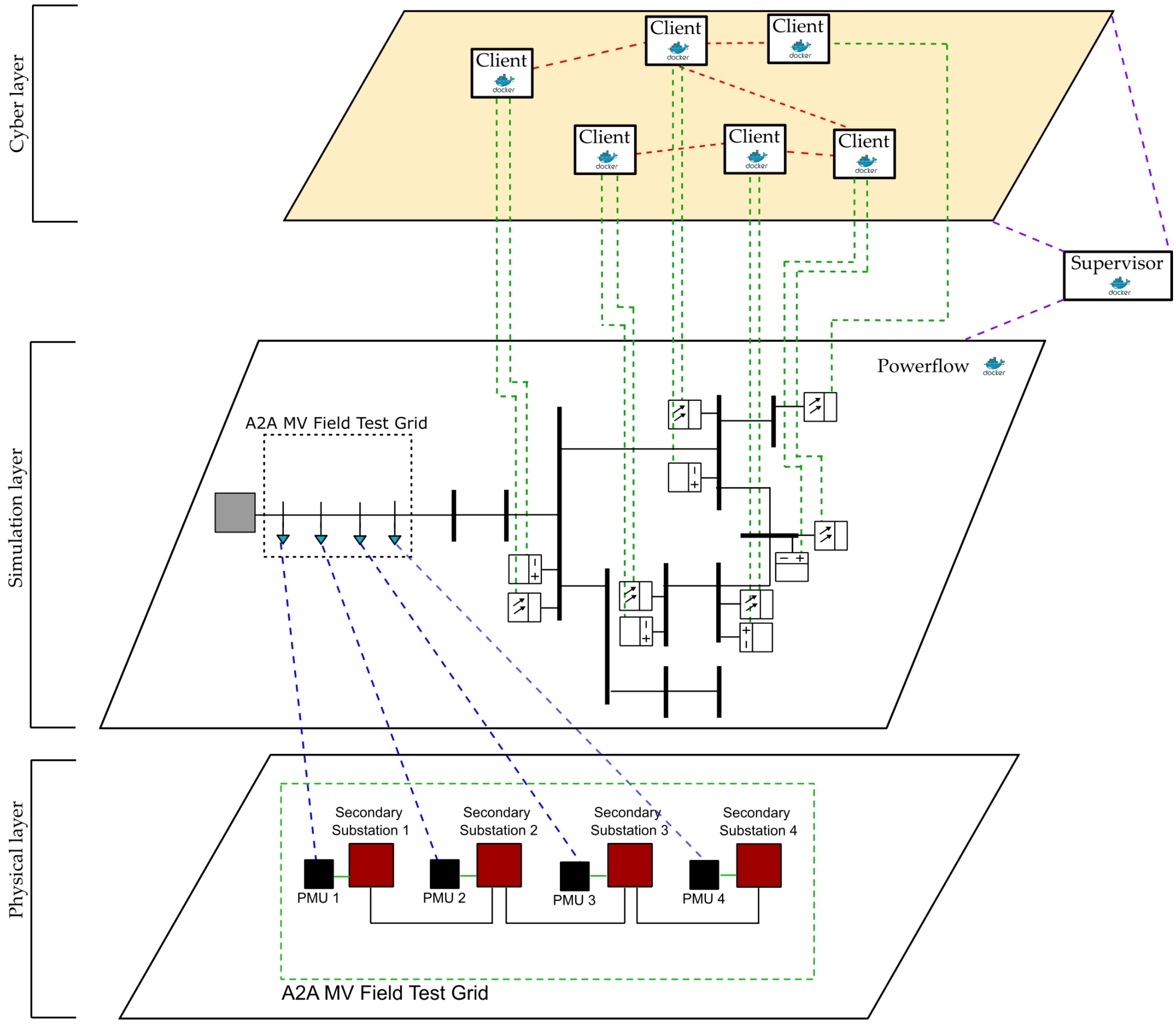

Figure 12 Description of the simulated field trial with the integration of the measurements from the field.

The initialization of the control is an important step to perform the simulation test and it is composed of several elements:

- **User**: It has direct command of the initialization of the operation and can always stop the operations of one or multiple *Clients*.
- **Docker compose**: Represents a tool provided by Docker that can be used to define services to be instantiate in several containers.
- ***Supervisor***: Performs the registration and initialization of the *Clients* and monitors the status of the cyber layer.
- ***Client*** j: Is the j-th controllable node instantiated in a software container.
- **Powerflow**: Software container performing the simulation of the grid.
- **Real System**: Real data obtained from the grid.

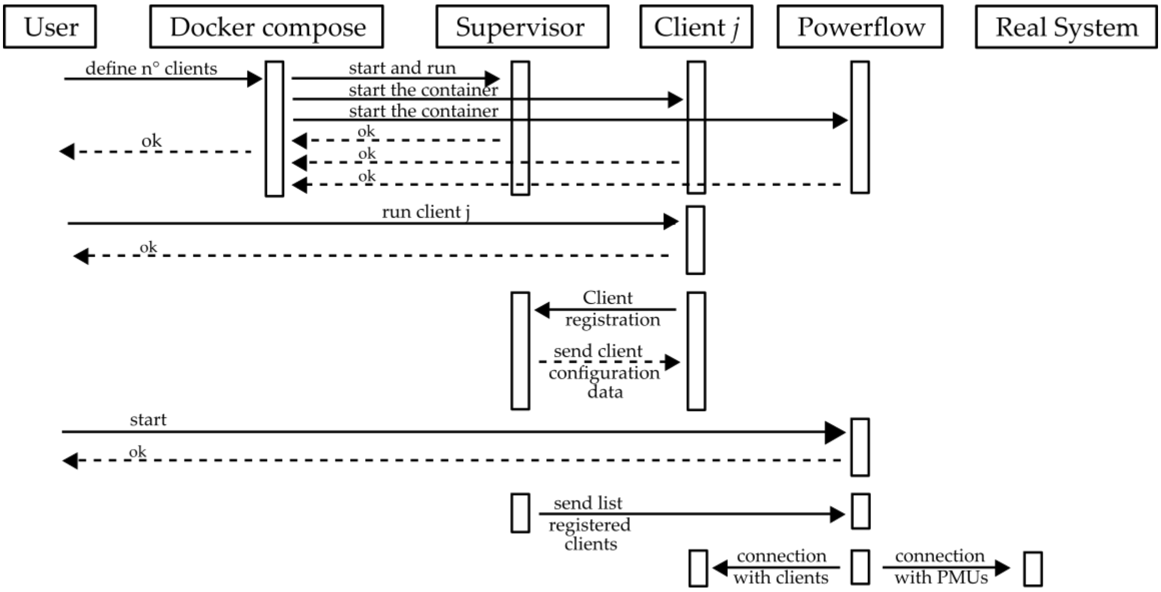

Figure 13 Initialization of the Distributed Control

To initialize the cyber layer, the user specifies the number of clients and runs the docker-compose file. This triggers the docker engine to instantiate the Supervisor, Clients, and Powerflow containers. Once the containers are up and running, the Clients send a JSON message containing their hostnames to the Supervisor, which collects this information and registers the Clients.

The algorithm that describes the registration of the *Clients* is presented in Figure 14, which shows that when a new *Client* is registered, the vector $\boldsymbol{reg_s}$, representing the registry of the all the Clients is modified. The registration of the new *Client* results in the recalculation of the graph $\mathcal{G}$ (based on the algorithms Annex A.1.2.1 and A.1.2.2), the matrix G and the control parameters α, γ.

Algorithm Registration of *Client h*

open the HTTP port for *Clients* registration
while True **do**
  Place any newly registered *Client* in $\mathbf{reg}_s$
  if $\mathbf{reg}_s$ not none **then**
    if $\mathbf{reg}_s \neq \mathbf{reg}_{s-1}$ **then**
      Update $\mathbf{G}, \mathcal{G}$
      Update $\boldsymbol{\alpha}, \gamma$
      for h in $\mathbf{reg}_s$ **do**
        Send $\boldsymbol{\alpha}[h], \gamma, \mathbf{G}[h,:], \mathcal{G}[h,:]$ to *Client h*
      end for
    else
      No *Clients* registered
    end if
  end if
  $s = s + 1$
end while

Figure 14 Algorithm for the registration of the *Clients*

After the initialization of the *Clients* the simulation of the electrical grid in the Powerflow container is initialized. Once the simulation is initialized, the *Supervisor* sends the registry of registered *Clients* to identify to which containers the measurements are sent, and the control set-points received.

In addition to the HTTP connection with the *Clients* the Powerflow container connects to the MQTT broker for the integration of the measurements from the field.

4.3 Description of the tests and results

This section describes the tests conducted to validate the proposed implementation of the distributed algorithm, which aimed to ensure that the voltage remains within the limits and to confirm the suitability of the software container-based implementation. The tests included the coordination of PVs and ESSs, the activation of control nodes using lagrangian multipliers, the scalability of the algorithm, and the interaction between DSO and customer assets.

4.3.1 Coordination of Reactive and Active Power control

To coordinate control actions, the parameter α can be used to prioritize the absorption or injection of active or reactive power in a node where both resources are available. To prioritize the use of ESSs, α can be set to activate reactive power control of a node only when the injection or absorption of active power of ESSs installed in neighboring nodes has reached their limits. By doing so, the prioritization is defined at the local level, allowing customers to exploit one resource only, if desired.

In the test, the load consumption is kept constant to a value in per unit of $0.3\ [p.u.]$. The PV generation is considered increasing from a value of $0.8\ [p.u.]$ to a value of $1.1\ [p.u.]$, which generates an overvoltage condition in the simulated grid. The results prioritized control of the active power of the ESSs is described in Figure 15 , whereas the control of the reactive power control is described in Figure 16 (where iterations define the number of iterations of the powerflow simulator).

The two figures clearly show that the reactive power injection in node 14 and 15 is activated only at iteration 117 because the active power injection of the ESSs of node 14 and 15 has reached the limit. Therefore, given that for both node 14 and 15 at least one neighbor has reached the limit, the reactive power control is activated, by changing the value of the parameter α. The resulting control actions can be also compared with Figure 29 and Figure 30 in the Annex A.1.3, where the resulting control set-points without the prioritization are described.

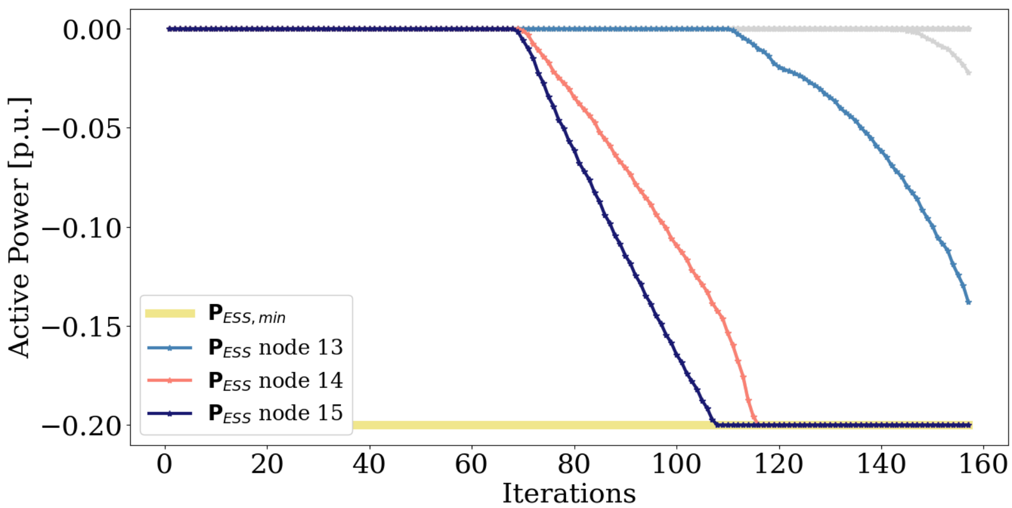

Figure 15 Active power control of the ESSs with prioritization

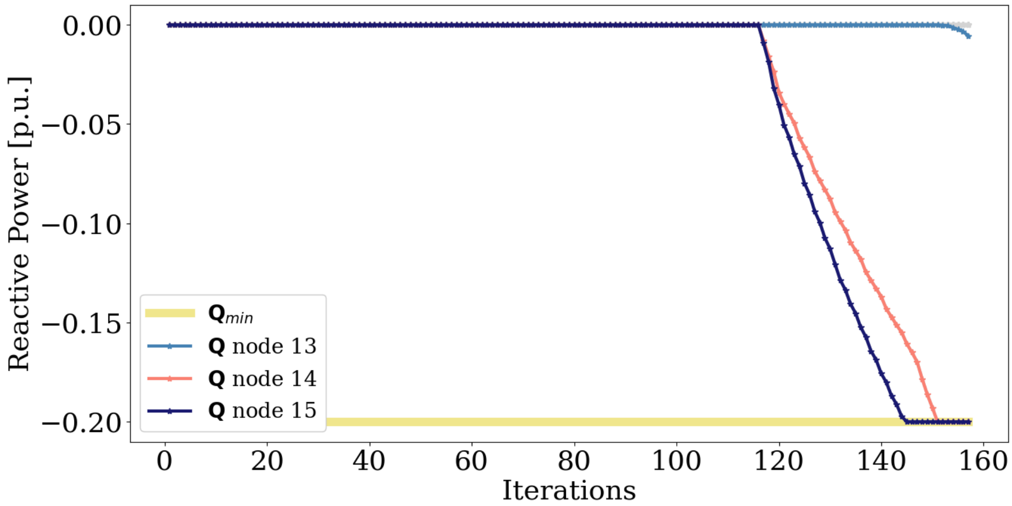

Figure 16 Reactive power control of the PVs with prioritization

Moreover, the prioritization of the active power control guarantees a reduction of the losses with respect to the case without prioritization, as described in Figure 17.

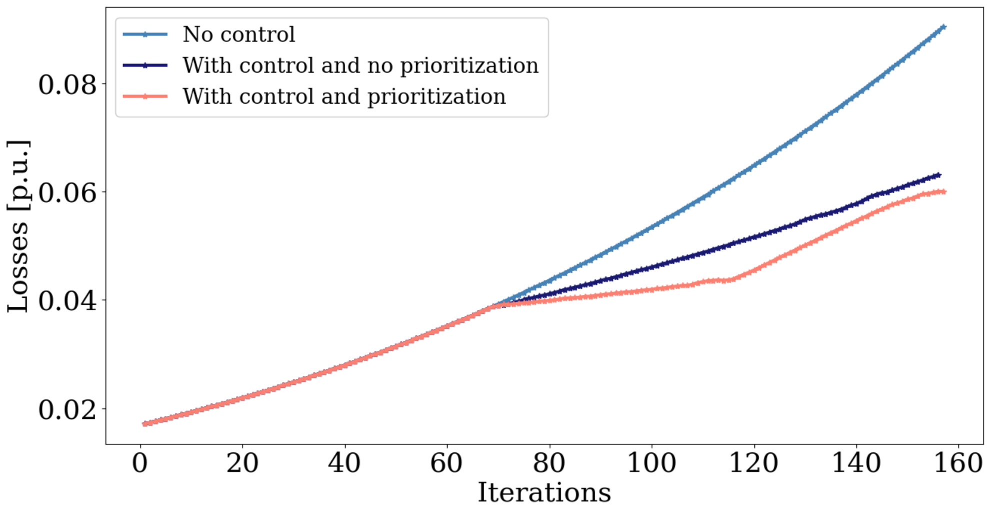

Figure 17 Total losses in the distribution grid

The percentage of losses reduction with respect to the uncontrolled scenario within 160 iterations of the powerflow simulations are displayed in Table 2.

Table 2 Total losses percentage reduction

No Control	Control with no prioritization	Control with prioritization
0%	16%	19%

This first test has demonstrated that the prioritization of the different assets installed in the grid can be performed directly modifying the control parameters of the distributed algorithm, without involving any additional coordination algorithm. Furthermore, this is performed directly at the control node level, without a centralized coordination.

4.3.2 Coordination of the control nodes via communication

Another important feature of the distributed implementation is that activation of the control actions of the different control nodes is triggered by the communication of the lagrangian multipliers. This approach guarantees a coordination among the control nodes that the decentralized implementation cannot provide.

To test the coordination, the same simulation scenario presented in Section 4.3.1 has been applied, where only two control nodes, namely 15 and 11 are activated. With this configuration it appears clear that an overvoltage measured in node 15 could not be seen in node 11, especially in a condition of increasing generation. However, thanks to the communication, node 11 starts absorbing active power at iteration 90, because node 15 reaches the limit.

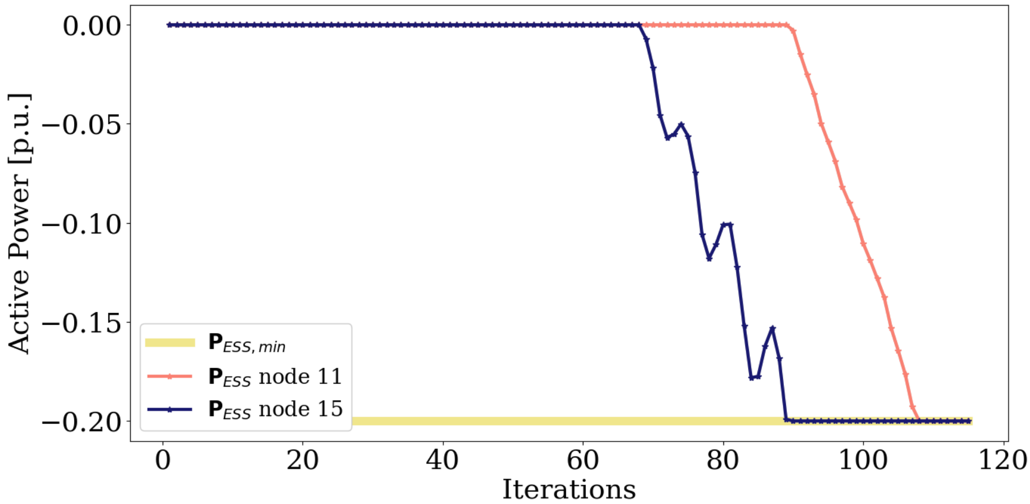

Figure 18 Active power control of the ESSs

Figure 19 shows that at iteration 90 node 11 is not measuring any overvoltage, demonstrating that the activation of the active power control of node 11 is only due to the communication of the lagrangian multipliers from node 15.

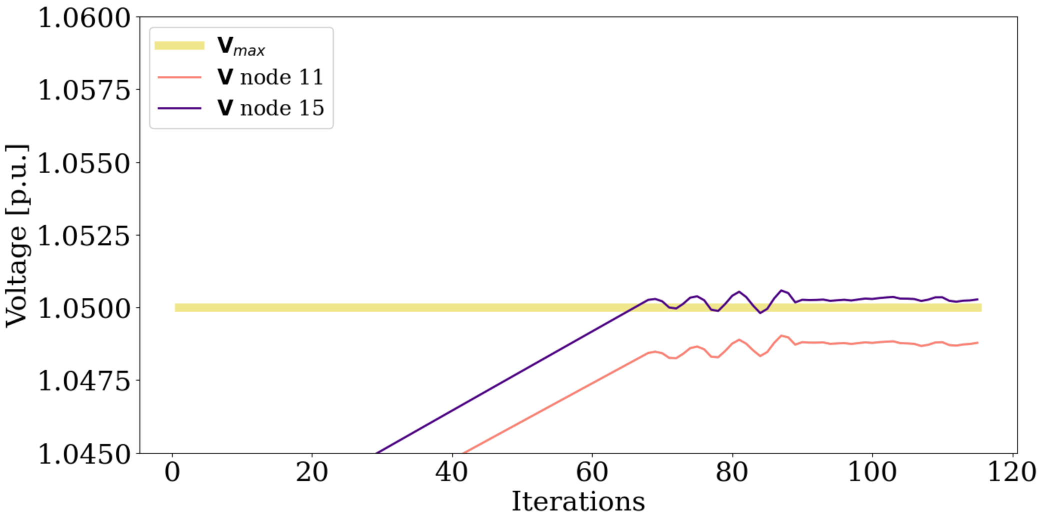

Figure 19 Voltage simulated values

4.3.3 Scalability

As the proposed algorithm is distributed, it is important to evaluate its scalability when applied to a large-scale system. As described in the results in Section 4.3.2, the activation of the control action in neighboring nodes is related to the communicated lagrangian multiplier values, which are directly linked to the limit values of power injection or absorption. Therefore, the algorithm exhibits a cascading behavior, meaning that not all nodes are simultaneously activated to control the voltage. This characteristic is an interesting feature for scalability, and the purpose of this test is to evaluate it while considering the real HTTP communication implemented within the Clients.

The implementation of the exchange of lagrangian multipliers in the Client is shown in Figure 20, which illustrates that the resulting local lagrangian multipliers are sent to neighboring nodes only if their values are greater than zero, reducing the need for communication.

Algorithm Solving Distributed Control on *Client* h

while True **do**
  Receive measurement $\mathbf{V}_k^h$
  Receive $\mathbf{G}_{hj}, \mathcal{G}_{hj}\,_{\mid j \in P_h}$, α, γ ▷ from *Supervisor*
  if $\mathbf{V}_k^h \neq None$ and $\mathbf{V}_k^h \neq \mathbf{V}_{k-1}^h$ **then**
    local calculation of lagrangian multipliers
    for $j \in P_h$ **do**
      if $\chi_{min,\mathbf{x}}^h(k+1) \neq 0$ or $\chi_{max,\mathbf{x}}^h(k+1) \neq 0$ **then**
        Send $[\chi_{min,\mathbf{x}}^h, \chi_{max,\mathbf{x}}^h](k+1)$
      end if
      Receive $[\chi_{min,\mathbf{x}}^j, \chi_{max,\mathbf{x}}^j](k+1)$
    end for
    calculation of control output
    $\hat{\mathbf{x}}^h(k+1) = \mathbf{x}_{min}^h \leq \mathbf{x}^h(k+1) \leq \mathbf{x}_{max}^h$
    Send $\hat{\mathbf{x}}^h(k+1)$ to physical layer
  end if
  $k = k + 1$
end while

Figure 20 Algorithm for the calculation of the control output

The test on scalability required an extension of the grid used for the previous test, which is represented in the CIGRE MV Test Grid has been replicated four time, connecting node 15 with node 5 of the following copy of the grid. The resulting grid consists of 45 grid nodes with 24 control nodes placed in the cyber layer. The control nodes are therefore placed in the following nodes:

- Area 1: [7,11,12,13,14,15]
- Area 2: [17,21,22,23,24,25]
- Area 3: [27,31,32,33,34,35]
- Area 4: [37,41,42,43,44,45]

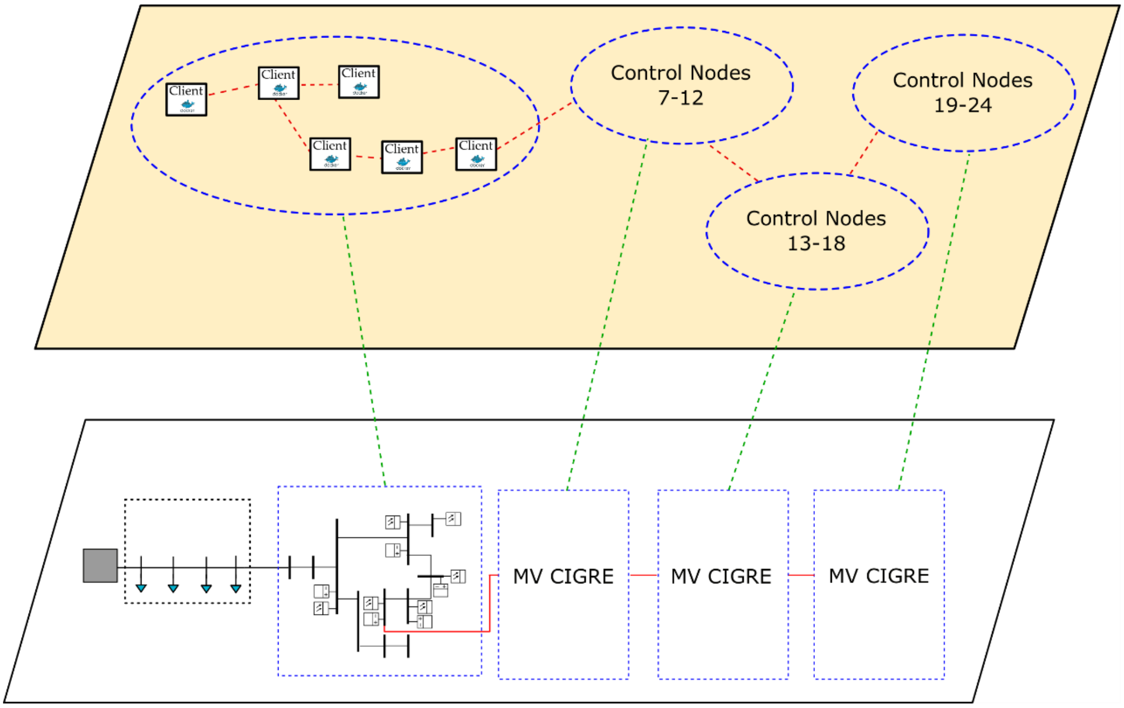

Figure 21 Extended simulation environment and cyber layer

The test has been performed with different level of percentage of overvoltage, defined as:

$$max_{\Delta V\%} = \frac{\max(V^k)}{V_{max}} \cdot 100$$

where $\max(V^k)$ represents the maximum value of measured overvoltage and V_{max} the overvoltage limit. In the test, the total amount of packets exchanged during the first 100 seconds of the simulations among the control nodes is calculated for different values of $max_{\Delta V\%}$, as described in Figure 22.

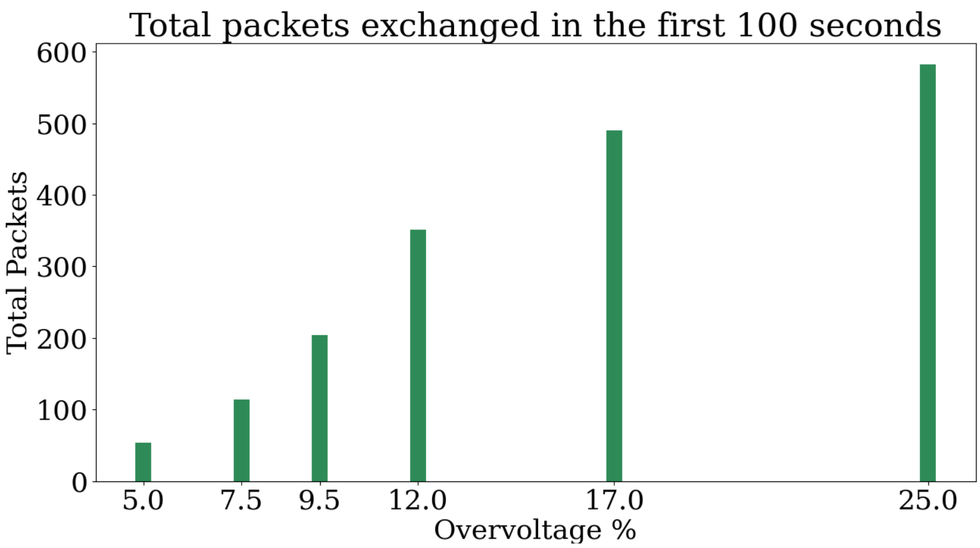

Figure 22 Total number of packets exchanged in the first 100 seconds

The figure shows how the number of packets exchanged with the increase of the overvoltage level, because more nodes have reached their maximum value. This can be seen in Figure 23, which shows the result with 12 % of overvoltage. In this configuration, only the last five control nodes reach their limits and therefore start exchanging the lagrangian multipliers with their neighbors.

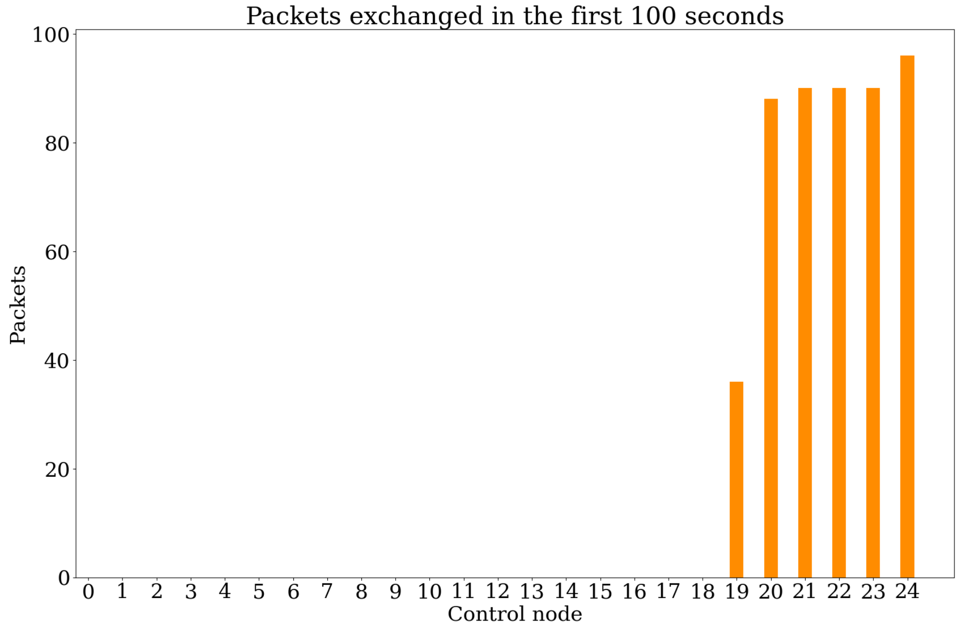

Figure 23 Number of packets exchanged in the first 100 seconds for each control node

The results of this test show that the control algorithm is scalable given that the communication among the control nodes is independent from the total amount of controllable nodes, but it only depends on the number of nodes that have reached their limits.

4.3.4 Interaction of DSO and Customers' assets

The final test is meant to identify and measure the positive contribution that the involvement of customers could have with respect to the reduction of the direct use of the DSO assets to control the voltage.

To perform the test, the same grid defined in Section 4.3.3 has been employed, where the control nodes have been equally divided in DSO and Customers' nodes as follows:

- DSO: [7,14,15,17,24,25,27,34,35,37,44,45]
- Customers: [11,12,13,21,22,23,31,32,33,41,42,43]

In the first test only the DSO nodes have been utilized, in a condition of overvoltage. The resulting active power set-points for the ESSs are described in the figure below.

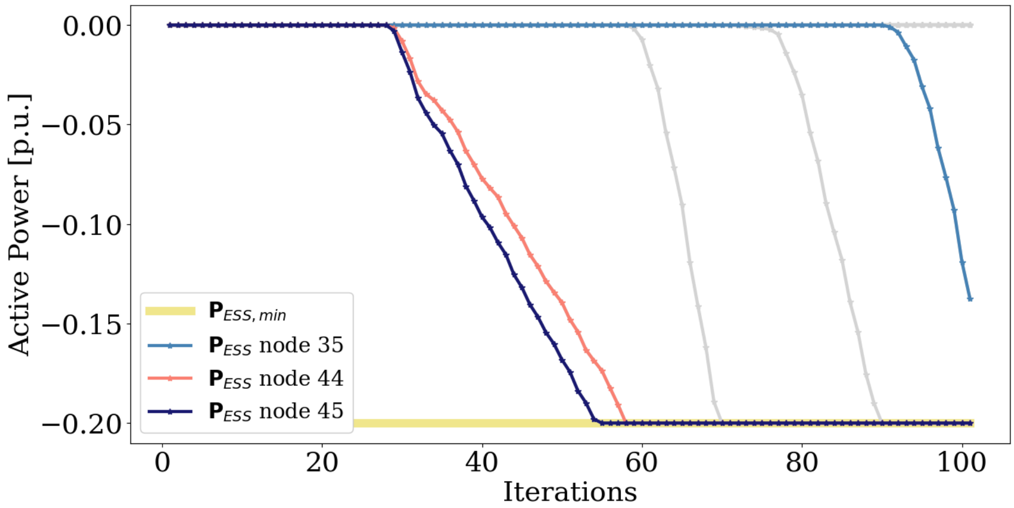

Figure 24 Active power control of the DSO ESSs

The second test is presented in Figure 25, which shows the active power absorption of the installed ESSs when both DSO and Customer's assets are utilized.

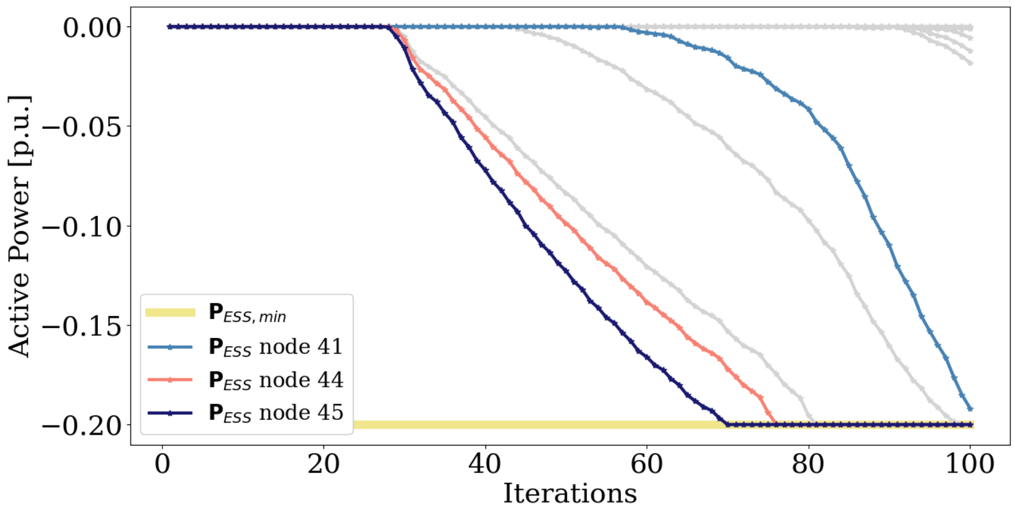

Figure 25 Active power control of the total ESSs (DSO + Customers)

The comparison of the two figures immediately highlights that the participation of the customers in the control of the voltage can drastically reduce the action of the DSO assets. In Figure 24 the control action of the ESS placed at node 35 is activated at iteration 91, whereas in Figure 25 the ESSs placed at node 41 is activated. Table 3 shows that the support of the customers helps reducing the activation of DSO assets by more than 50 %.

Table 3 Number of active DSO assets

	Control with only DSO assets	Control with DSO and Customer's assets
Active DSO assets	5	2

4.3.5 Exploitation of the results

The field trial generated a significant amount of data and results, including the evaluation of the PMU prototype, system accuracy, the digitization of the relevant grid section, and the results of the voltage control service. The DSO can use a considerable portion of these results to assess the benefits of implementing the edgeFLEX service in a larger part of their network. Based on a careful evaluation of the advantages and disadvantages, the DSO may also propose potential improvements to the overall system. Academic partners such as UNIBO and RWTH will consider the results as research outcomes, and new concepts and solutions will emerge from the trial results.

4.4 Dashboard for the visualization

Along with the implementation of the distributed algorithm, a dashboard interface for visualization has been created. The dashboard, built using the Grafana dashboard software, enables online visualization of the data obtained from the edgePMUs installed in the grid. With the dashboard, users can directly view the status of the grid.

Figure 26 Dashboard for the visualization of the edgePMU data

The overall dashboard is presented in Figure 26, which displays the data from three of the four installed edgePMUs for visualization purposes. Since the edgePMUs provide timestamped data, the received information can also be viewed in terms of collected data over time, as shown in in Figure 27 and Figure 28, displaying the voltage and frequency profiles, respectively. This configuration enables users to visualize the voltage and frequency dynamics within a specific time range, as the data can be stored in a database or file. This provides the ability to conduct further analysis based on historical data.

Figure 27 Voltage magnitude profiles obtained from three edgePMUs for 25 minutes

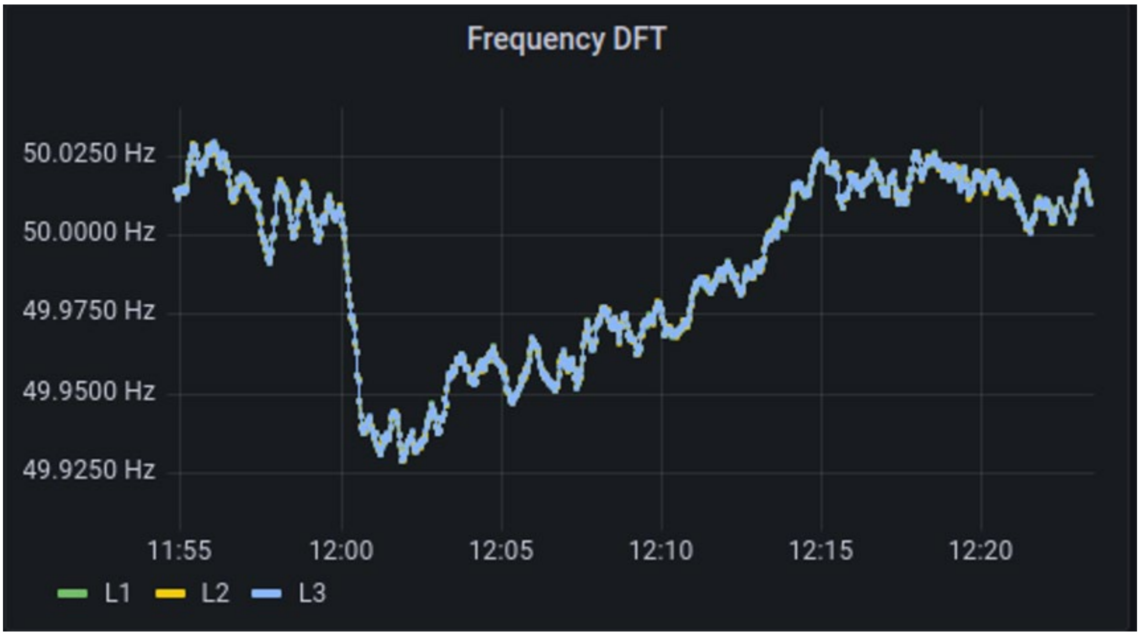

Figure 28 Frequency profiles obtained from three edgePMUs for 25 minutes

4.5 Conclusions

This chapter presents the implementation and tests of distributed voltage control in an Italian field trial. To compensate for the lack of controllable devices and the small size of the grid, the model was extended with a reference grid where controllable PVs and ESSs were simulated, and measurement data from the field was integrated. The distributed algorithm was briefly described in Section 4.2.3, while the implementation with Docker containers is detailed in Section 4.2.4. This implementation of distributed control using Docker containers and the interface with the powerflow simulator led to the creation of a CPS where measurements obtained from edgePMUs were integrated.

Tests performed in Section 4.3 demonstrated the algorithm's ability to coordinate and prioritize resources without central coordination, relying only on communication of the lagrangian multipliers. Communication of the lagrangian multipliers was also tested to demonstrate the algorithm's ability to activate neighboring nodes, even if these nodes are not directly measuring any voltage problem. An extended grid was used to test the scalability of the algorithm, proving that node activation depends only on the value of overvoltage, not on the overall installed PVs or ESSs. Finally, coordination of DSOs and customer assets was tested, showing how customer participation can reduce the DSO's commitment to solving voltage problems in the electrical grid. This conclusion supports the conclusions of the edgeFLEX field trial undertaken in the SWW network in Wunsiedel, Germany and reported in D5.4.

5. Conclusion

The Italian field trial was the only one hosted by an external DSO. Consequently, many more difficulties were faced during the trial design and development, but they were all solved. Thanks to the collaboration between the partners and the DSO, several results were obtained. The results of the Italian field trial can be summarized as follows:

- External DSO. The trial demonstrates that the topics studied in the edgeFLEX solutions are of considerable interest to DSOs that were not members of the consortium and that DSOs were willing to join the field trials at their own expense.
- Ease of integration. The HW and SW needed to implement the edgeFLEX services were integrated in the complex DSO's architecture. Of course, some adaptation was needed to match the existing equipment with the new equipment.
- Validation of the edgePMU. The laboratory and field testing of the edgePMU confirmed its performance compared to commercial devices. The cost of the commercial devices is between one and two orders of magnitude higher than the cost of the edgePMU.
- Voltage control service. It was demonstrated that it is possible to implement the voltage control service, and its benefits, by using the measurements collected from the field.
- Digital Twin. The collaboration between the DSO and the edgeFLEX partners enabled the project to make a further advance. The digitalization of the portion of grid considered in the field trial enabled the development of a simplified version of a digital twin of this network segment. The implementation of the digital twin provides the basis for a variety of applications such as predictive maintenance, fault prediction and accuracy evaluation.

6. List of Tables

7. List of Figures

8. References

Commision, E. (2022). *Digitalisation of the energy system*. Retrieved from https://energy.ec.europa.eu/topics/energy-systems-integration/digitalisation-energy-system_en

Council, E. (n.d.). *Cybersecurity: how the EU tackles cyber threats*. Retrieved from https://www.consilium.europa.eu/en/policies/cybersecurity/

De Din, E., Pau, M., Ponci, F., & Monti. (2007). , A. A Coordinated Voltage Control for Overvoltage Mitigation in LV Distribution Grids. Energies 2020, 13,.

Docker. (2022, 01). *Use containers to Build Share and Run your applications,* . Retrieved from https://www.docker.com/resources/what-container.

E. De Din, M. P. (n.d.). Implementation of the online distributed voltage control based on containers. *2022 International Conference on Smart Energy Systems and Technologies (SEST), 2022, pp. 1-6, doi: 10.1109/SEST53650.2022.9898150.*

Farivar, M. a. (n.d.). "Branch flow model: Relaxations and convexification—Part I." IEEE Transactions on Power Systems 28.3 (2013): 2554-2564.

NetwrokX. (n.d.). *NetwrokX*. Retrieved from https://networkx.org/

POLITICO. (n.d.). *Physical attacks on power grid surge to new peak*. Retrieved from https://www.politico.com/news/2022/12/26/physical-attacks-electrical-grid-peak-00075216

PYPOWER. (n.d.). Retrieved from https://pypi.org/project/PYPOWER/

Resources, B. S. (2018). (CIGRE) Retrieved from https://e-cigre.org/publication/ELT_273_8-benchmark-systems-for-network-integration-of-renewable-and-distributed-e

9. List of Abbreviations

PMU	Phasor Measurement Unit
DSO	Distribution System Operator
DMS	Distirbuted Measurement System
DG	Distributed Generator
LV	Low Voltage
MV	Medium Voltage
MQTT	Message Queue Telemetry Transport
CPS	Cyber Physical System
HTTP	Hypertext Transfer Protocol
ESS	Energy Storage System
PV	Photovoltaic

ANNEX

A.1 Annex chapter 4

A.1.1 Grid data

Table 4: Grid data of the A2A MV Field Test Grid

IN	OUT	Length [km]	R (ohm)	X (ohm)	R (p.u.)	X (p.u.)
1	2	0,016	0,003296	0,001728	0,000082	0,0000432
2	3	0,013	0,002678	0,001404	0,000067	0,0000351
3	4	0,008	0,001648	0,000864	0,000041	0,0000216
4	5	0,011	0,002266	0,001188	0,000057	0,0000297

Table 5: Grid data of the CIGRE MV benchmark Grid

IN	OUT	R (p.u.)	X (p.u.)
5	6	0,009064	0,004752
6	7	0,0035	0,005
7	8	0,0035	0,005
8	9	7,51E-04	0,0012
9	10	7,51E-04	0,0012
7	12	0,0019	0,0027
12	11	0,0016	0,0023
12	13	0,0021	0,003
13	14	3,75E-04	5,36E-04
14	15	0,001	0,0014

A.1.2 Graph algorithm

A.1.2.1 For PVs

```
Gx = nx.from_numpy_matrix(G)
            graph_DG = {}
            for i in range(len(self.num_pv)):
                neigh = []
                for j in list(Gx._adj[i].keys()):
                    if j!=i:
                        neigh.append(j)
                    else:
                        pass

                graph_DG.update({"node"+str(i): neigh})
```

A.1.2.2 For ESSs

```
BESSx = nx.from_numpy_matrix(B_ess)
            graph_ESS = {}
            for i in range(len(self.num_ESS)):
                neigh = []
                for j in list(BESSx._adj[i].keys()):
                    if j!=i:
                        neigh.append(j)
                    else:
                        pass

                graph_ESS.update({"node"+str(i): neigh})
```

A.1.3 Additional results

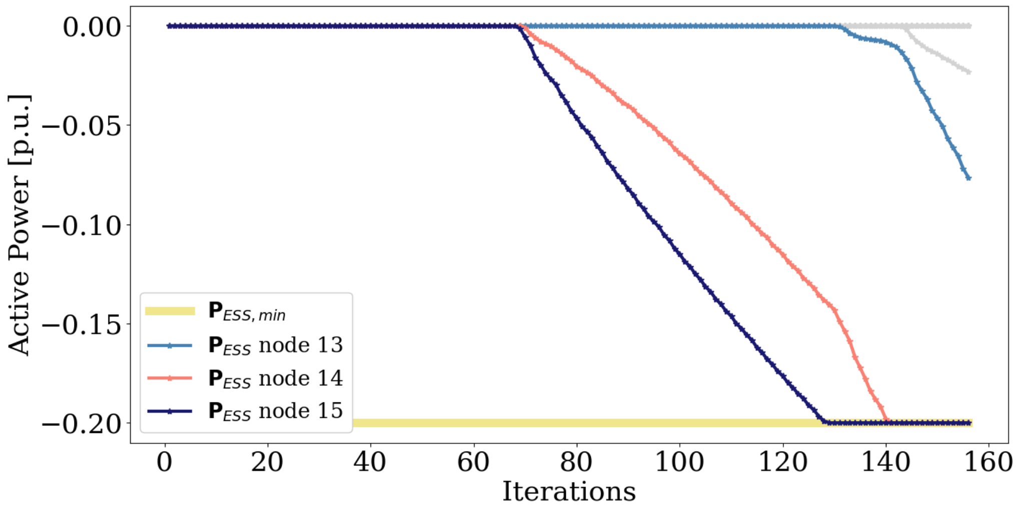

Figure 29 Active power control of the ESSs without prioritization

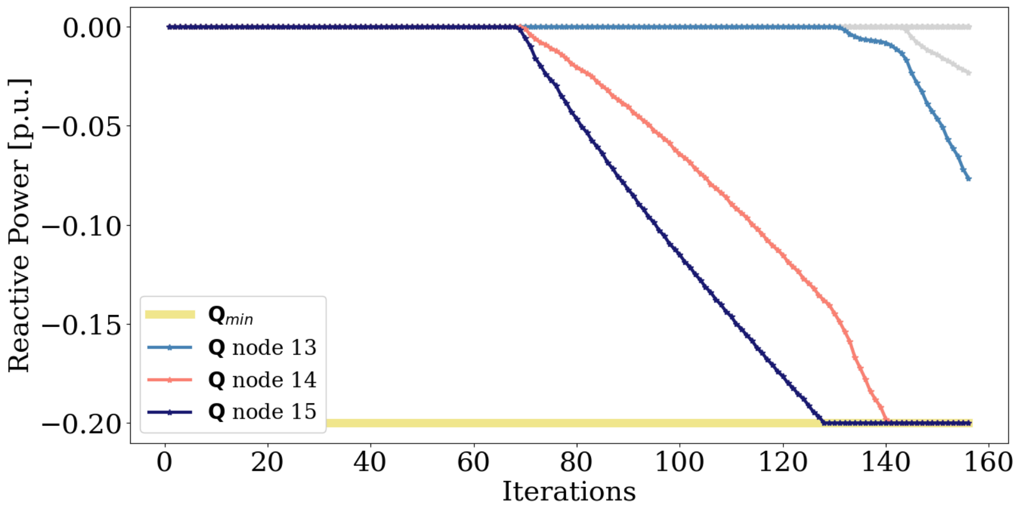

Figure 30 Reactive power control of the PVs without prioritization